Available online at http://proceeding.rsfpress.com/index.php/ess/index
LPPM UPN "Veteran" Yogyakarta Conference Series
Proceeding on Engineering and Science Series (ESS)
Volume 1 Number 1 (2020): 385-396

Spatial filtering of Time Domain Induced Polarization (TDIP): Enhancement of spatial estimates of Mineralization at Gunung Parang Karangsambung Kebumen, Central Java

Wrego Seno Giamboro , Wahyu Hidayat

Universitas Pembangunan Nasional Veteran Yogyakarta
[1]Email address wrego_seno@upnyk.ac.id [2]Email address Wahyu.hidayat@upnyk.ac.id

Abstract

Geophysical data acquisition is principally a function of spatial frequency. In some cases, geophysical acquisitions require enough space to obtain detailed information. However, in certain conditions, such as limited measurement instruments and conditions in the research area, this cannot be done. Several ways can be applied, such as improvisation during data acquisition or when processing data. In this study, a spatial frequency data processing approach has been carried out, which aims to enhance and obtain target anomalies more clearly using spatial filter analysis. The target of this research is the mineralization zone in Mount Parang Karangsambung, Kebumen Regency, Central Java, using the Time Domain Induced Polarization method with four lines using a Dipole-dipole configuration with a measuring spacing of 10 meters. The output of this research is to compare the real data processing of 10 meters spatial field with spatial filter processing to be 5 meters. The processing results show an increase in the sharpness of the resistivity and chargeability images on the 5-meter spatial data. There was an increase in the target image, namely mineralization, as indicated by the response of contrast resistivity and chargeability. The use of spatial filters can increase the resolution of the resistivity and chargeability sections so that the lithology and mineralization zone can be well defined.

Keywords: Spatial analysis, Induced Polarization, Enhancement

I. INTRODUCTION

Instrumentation is the main tool of geophysicists. Instrumentation with high precision and accuracy will get better data. Geophysical survey measurements are now made easy with the use of automated instrumentation. In some cases of instrumentation, such as the Time Domain Induced Polarization (TDIP) method, the distance between the current and potential electrodes is crucial (Alhassan et al,

2015) The closer the spacing between the electrodes, the more detailed the mapping results will be (Day-Lewis,2005). However, there are times when the instrumentation is not only easy but also an obstacle (] Johansson and Flyhammar,2007). As an example of TDIP instrumentation, the distance between the electrodes has been determined at a certain distance. In today's modern instrumentation, the distance between the electrodes has been set as short as 10 meters to 20 meters (Richards et al, 2017, Uhlemann, 2017). This setting results in less than optimal resolution results due to electrode distance setting. In this study, an approach has been made to overcome the limitations of instrumentation using spatial filters when processing data (Loke, 2004) . Measurement data with a certain distance is filtered using a spatial filter reaching ½ electrode spacing. The aim is to see the difference in resolution between electrode spacing between real measurements and filter treatment.

This research was conducted in the area of Mount Parang Karangsambung, Kebumen Regency, Central Java, using data from 4 measurement lines with 10 meters between electrodes, and the configuration used was the Dipole-dipole configuration. The dipole-dipole array was chosen as it is known to provide high-resolution data while effectively exploiting multichannel measurement systems (Chambers , 2014, Dahlin and Zhou, 2004, Loke, 2004) Mount Parang is thought to be the result of a magmatic intrusion, which is thought to be a continuation of the magmatic route of the southern islands of Java and Sumatra (Asikin, 1974).. Diabase Gunung Parang is an alkaline igneous rock that is rich in dark Fe content, which was formed as a result of collisions between continental plates and oceanic plates that occurred during the Miocene period (Prasetyadi, 2006). A side product of intrusion is the potential for mineralization. In this study, the prospect of mineralization will be examined using the TDIP method with a real measuring spacing of 10 meters and the processing results using a spatial filter in half, and the resolution analysis is carried out.

II. LITERATURE REVIEW

Mount Parang is one of the Karangsambung Geopark sites. The Lok Ulo melange complex area itself has become a geological reserve through a decree of the Minister of Energy and Mineral Resources of the Republic of Indonesia No. 2817K / 40 / MEM / 2006, which was passed on November 10, 2006 . This ministerial decree protects the Lok Ulo melange complex from mining activities that can damage the geological reserve, which holds a variety of geological knowledge regarding the geological history, especially in Java and its surroundings (Figure1). The Karangsambung Geological Nature Reserve is in Karangsambung District, Kebumen Regency, Central Java Province, Indonesia. The northern boundary of this area is the Banjarnegara area, the east is bordered by the Wadaslintang area, the south is bordered by the Kebumen area, and in the west is the Gombong area. Geographically, the coordinates of the Karangsambung area are located at 07^o 34' 00"LS - 07^o 36' 30" LS and 109^o 37' 00" BT - 109^o 44' 00" BT. Physiographically, the Karangsambung area is included in the South Serayu Mountain Zone.

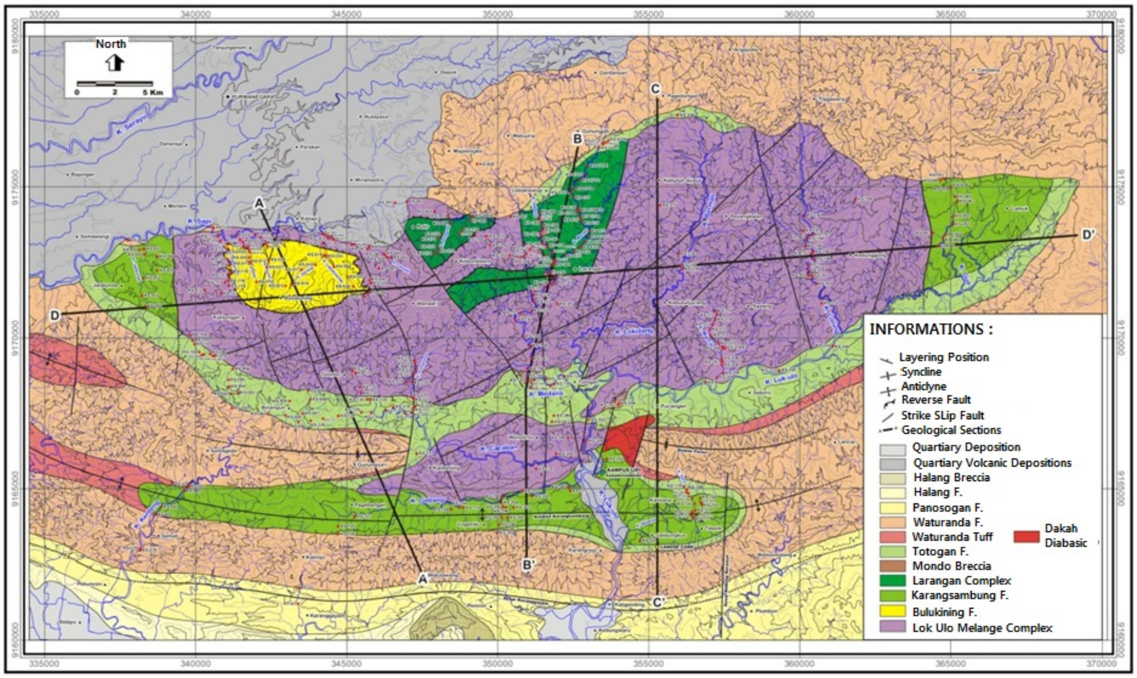

Figure 1. Geological map of Lok Ulo Complex (Prasetyadi et al, 2006)

Mount Parang is the result of a magmatic intrusion. To determine the potential for mineralization on Mount Parang (Alhassan, 2015, Asikin, 1974) , the TDIP method has been acquired with a Dipole-dipole configuration. The limitations of modern equipment require attacking geophysicists to be able to adapt to the conditions of the equipment and its working place (Purwanto, et al, 2020). The limitation of measurement spacing (distance between electrodes) in modern tools results in differences in resolution. To overcome this, an approach in data processing is needed so that it can increase data resolution.

III. RESEARCH METHODOLOGY

III.1. Time Domain Induced Polarization

The Time Domain Induced Polarization (TDIP) method can be applied to metal mineral exploration because it can identify rock polarization based on its chargeability (Lowry, 2007, Purwanto, 2020) . Mineralization exploration generally uses two methods, namely the resistivity method and IP (Telford, 1990) When the current is injected and turned off in a medium, the flowing ions will stop moving and return to their initial position (Kemna, et al, 2002) There is a difference in the travel time to the initial position (Johansson and Flyhammar, 2007, Telford, 1990.) The longer the rock keeps the electric voltage, the more conductive the rock will be (Chambers, 2014) In principle, IP measurement is divided into two methods, namely the frequency domain and time domain method (Telford, 1990). In this study, we are using the time-domain method.

TDIP is by flowing rectangular electric current pulses into the ground. When the electric current has stopped, the potential between the two measuring electrodes immediately drops to the secondary response level. This secondary potential then decays with time (Sumner, 1976) Measurements in the time domain have a charge ability quantity, which is a quantity indicating secondary potential decay with respect to time. This quantity shows potential decay properties that reflect the degree of polarization in a medium (Figure 2). Theoretically defined:

$$M = \frac{1}{Vp} \int_{t_1}^{t_2} Vs(t) dt$$

M: chargeability (msec) atau (mV/V), Vp : Primer Voltage (mV), and Vs = Secunder Voltage (mV)

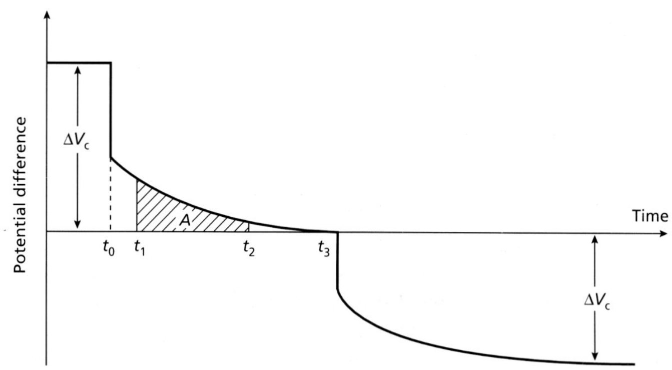

Figure 2. Potential decay response to time (Reynolds, 1997)

Measurements were carried out in 6 lines using a 10-meter spaced dipole-dipole configuration with varying lengths of length 300 meters. Field data from the measurement results obtained the value of voltage and current and the value of charge ability. The data is then processed using equations involving geometric factors; the goal is to get a value that is proportional to the current injected with the measured voltage. The results obtained are apparent resistivity and apparent charge ability. From the apparent resistivity data, a further process is carried out, namely the inversion process for each path. Interpretation is made by correlating the inversion 2D cross-section resistivity and changeability.

III.1.1. Filter Spatial (Half Spacing Filter)

A spatial filter, or also known as half spacing, is a filter that functions to change the measurement space in half. This aims to help users get more detailed data processing results. The principle of this method is to create a new data window between the used spaces and extrapolate between the closest data by tightening the existing grid/mesh, as shown in figure 3.

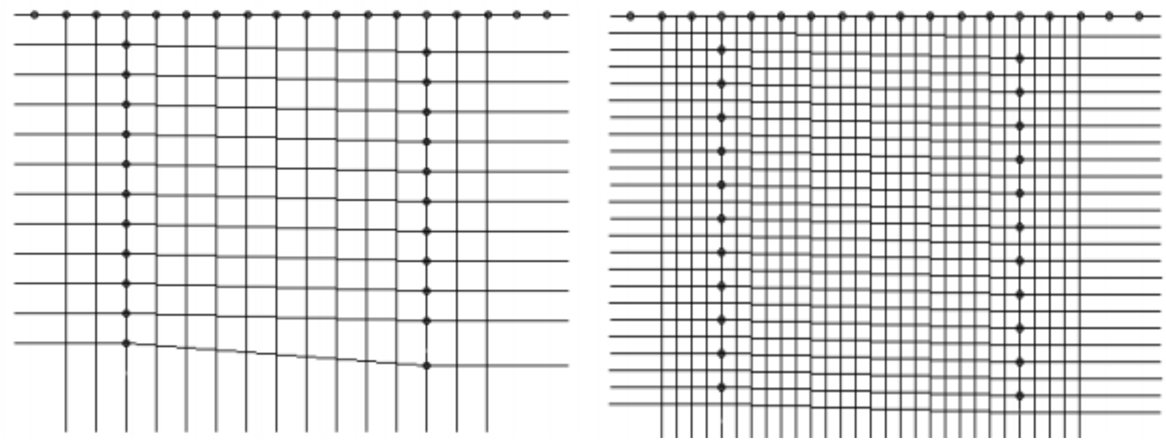

(a) (b)

Figure (a) Standard grid/mesh with specified spacing, (b) Grid/mesh half spacing (Loke, 2004).

The data from the measurement results are then calculated using a programming language and then inverted by the initial grid to the half spacing grid. At the time of inversion, the user can determine the iteration until the smallest Root Mean Square (RMS) value is obtained. The processing results are presented in the true resistivity and chargeability 2D section.

IV. RESULTS AND DISCUSSION

The data processing in this study is presented by comparing the two selected sections consisting of 2 and 3 trajectories. The data processing result is a real measurement using a space of 10 meters compared to the results of processed data using a spatial filter to 5 meters. Another cross-section can be seen in appendix 1. The results of data processing and comparison can be seen in Figures 4 to 7.

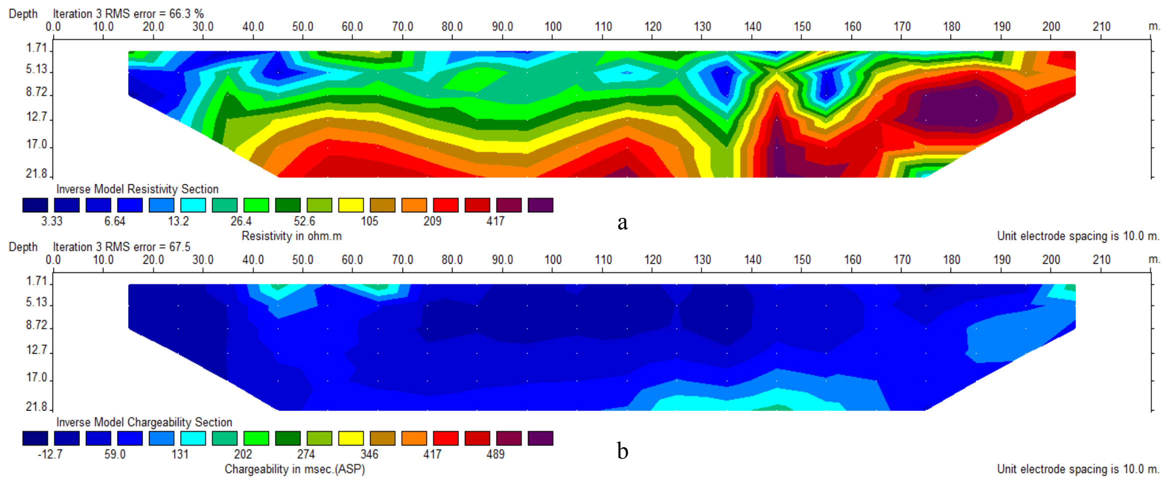

Figure 4. (a) The resistivity section (Ohm.m), (b) charge ability (msec) line 2 (space between electrodes 10 meters)

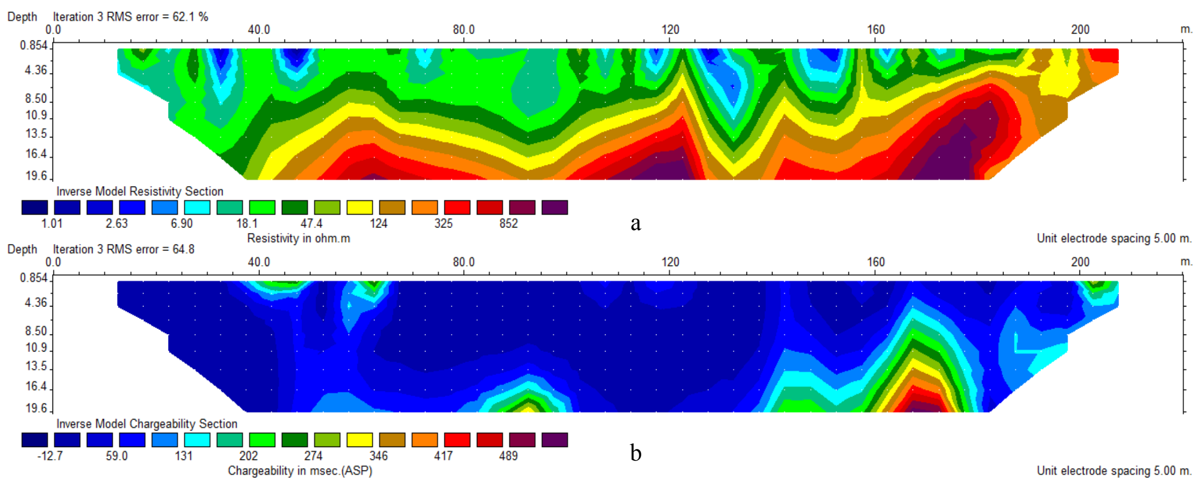

Figure 5. (a) The resistivity section (Ohm.m), (b) charge ability (msec) line 2 (space between electrodes 5 meters)

Figures 4 and 5 show the results of the measurement of the resistivity method as well as the TDIP at line 2.Figure 4 is a resistivity versus charge ability section with a measurement spacing of 10 meters, while Figure 5 is a resistivity versus charge ability section using a spatial filter to behalf of the real measurement electrode distance (5 meters). In Figures 4 and 5, the resistivity section (4a and 5a) can be seen that there is a resistivity contrast pattern. High resistivity contrast has been identified as an igneous rock intrusion. There was no significant difference between the resistivity sections 4a and 5a. Igneous intrusions were represented by high resistivity values of 300-5000 Ohm.m. The fundamental difference between these two resistivity sections (4a and 5a) lies in the measuring distance of 190 to 200 meters. The cross-sectional image of the intrusion rock 4a is visible to the surface, while the resistivity section 5a does not show the same thing. The resistivity section 5a shows that the intrusion rock is not continuous upward but is cut at a certain depth; the rock above it is indicated only a boulder which is cut with a weathered layer, which is indicated by a moderate resistivity value. In the chargeability section, it was found that there was a difference in contrast between the IP cross-sections of images 4b and 5b. In section 4b, there is no anomaly charge ability; in contrast to Figure 5b using a 5-meter space, the presence of mineralization is visible with a value of 300 - 600 msec. High mineralization zones can be seen at 80 to 100 meters at a depth of 15 to 20 meters and at a distance of 135 to 180 meters at a depth of 10 to 20 meters. This indicates the presence of metal mineralization in the intrusion of Mount Parang.

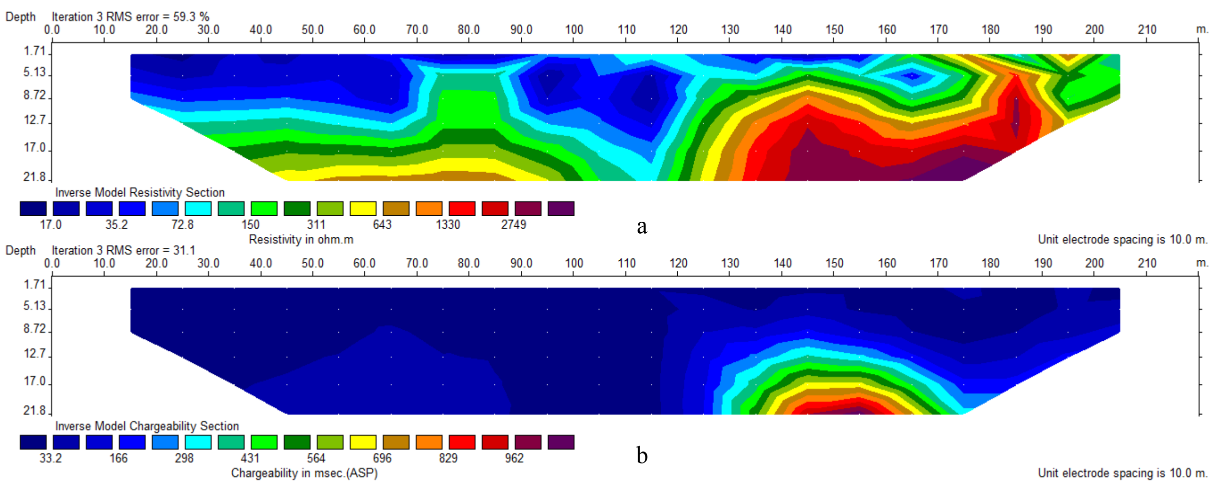

Figure 6. (a) The resistivity section (Ohm.m), (b) charge ability (msec) line 3 (space between electrodes 10 meters)

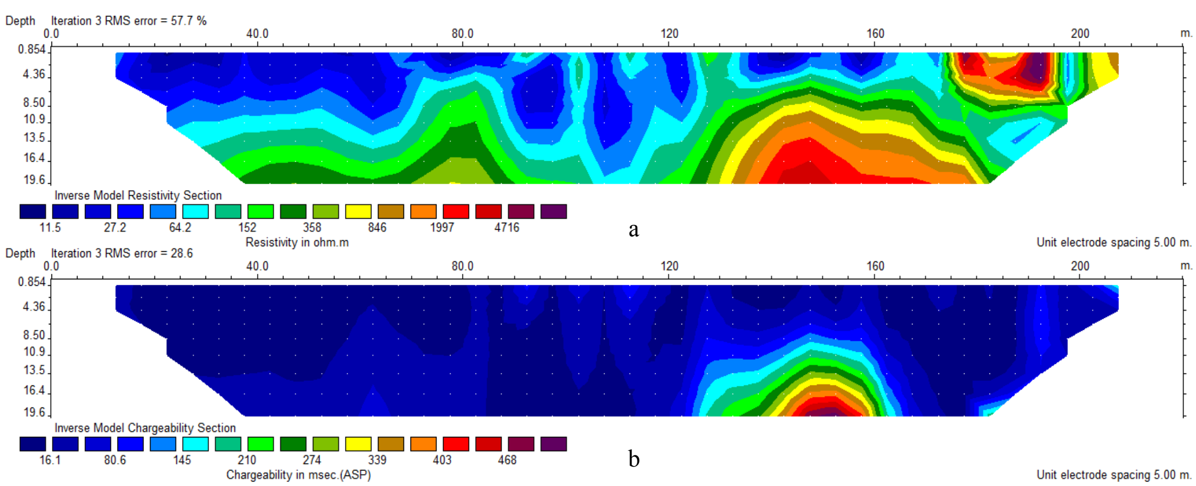

Figure 7. (a) The resistivity section (Ohm.m), (b) chargeability (msec) line 3 (space between electrodes 5 meter)

Figures 6 and 7 show the results of the measurement of the resistivity method as well as the TDIP at line 3.Figure 6 is a resistivity versus charge ability section with a measurement space of 10 meters, while Figure 7 is a resistivity versus charge ability section using a spatial filter to behalf of the real measurement electrode distance (5 meters). In Figures 6 and 7, the resistivity section (6a and 7a) can be seen that there is a resistivity contrast pattern. High resistivity contrast has been identified as an igneous intrusion. Igneous intrusions are represented by high resistivity values of 300-5000 Ohm.m. Similar to line 2, the contrast of the resistivity of the rocks is more visible in section 6a. Boulder and intrusion rock were separated in comparison with the 6a resistivity cross-section. In the chargeability section, there is a difference in the position of the chargeability contour, where the chargeability section 7a is shifted to the left at a measuring distance of 125 to 160 meters, while the figure 6a section is at 130 to 165 meters.

Based on the results of the resistivity and chargeability cross-sections, an important piece of information can be drawn about the body of the Mount Parang intrusion, namely that there is an indication of mineralization accompanying the Mount Parang intrusion process. This mineralization appears to fill gaps in the Mount Parang intrusion with an average depth of below 15 meters. The IP method with a space of 5 meters can show a good resolution; it can distinguish the differences between one rock body and another, and the presence of metal mineralization in the Mount Parang intrusion is quite good.

V. CONCLUSION

The conclusions of this study are:

1. The resistivity value of the Mount Parang intrusion rock ranges from 300 - 5000 Ohm.m, where the constituent lithology is diabase rock. The value of mineralization in the Mount Parang intrusion body is indicated by a high chargeability value of 300 - 600 msec, which indicates the presence of metal sulfide mineralization.
2. The use of spatial filters can increase the resolution of the resistivity and chargeability sections so that the lithology and mineralization zone can be well defined.

ACKNOWLEDGEMENTS

This study is carried out because of internal funding of internal fundamental research grant from Lembaga Penelitian dan Pengabdian Masyarakat (LPPM) UPN “Veteran” Yogyakarta, so that study can be carried out properly.

VI. REFERENCES

Alhassan, UD., Obiora, DN., Okeke, FN. (2015) The assessment of aquifer potentials and aquifer vulnerability of southern Paiko, Northcentral Nigeria, using the geoelectric method. *Glob. J. Pure Appl. Sci. 21:51-70.*

Asikin, S. (1974). Evolusi geologi Jawa Tengah dan sekitarnya ditinjau dari segi tektonik dunia yang baru. *Laporan disertasi, Dept. Teknik Geologi ITB*, 103.

Chambers, J.E., Gunn, D.A., Wilkinson, P.B., Meldrum, P.I., Haslam, E., Holyoake, S., Kirkham, M., Kuras, O., Merritt, A., Wragg, J., 2014a. 4D electrical resistivity tomography monitoring of soil moisture dynamics in an operational railway embankment. *Near Surf. Geophys*. 12, 61–72

Dahlin, T., and Zhou, B., 2004. A numerical comparison of 2D resistivity imaging with 10 electrode arrays. *Geophys. Prospect*. 52, 379–398.

Day-Lewis, F.D., 2005. Applying petrophysical models to radar travel time and electrical resistivity tomograms: resolution-dependent limitations. *J. Geophys. Res*. 110, B08206.

Johansson, S., Jones, S. and Flyhammar, F. (2007) Comparisons of 2D- and 3D-Inverted Resistivity Data As Well As of Resistivityand IP-Surveys on a Landfill, Near-surface, *13th European Meeting of Environmental and Engineering Geophysics*, Istanbul, Turkey, 3–5 September 2007, p. 42.

Kemna, A., Vanderborght, J., Kulessa, B., Vereecken, H. (2002). Imaging and characterization of subsurface solute transport using electrical resistivity tomography (ERT) and equivalent transport models. *J. Hydrol.* 267, 125–146

Keputusan Menteri Energi dan Sumberdaya Mineral RI No. 2817K/40/MEM/2006

Loke, M.H., 2004. *2D and 3D Electrical Imaging Surveys*. England: Birmingham University.

Lowrie, W. (2007). *Fundamental of Geophysic*. California: Cambridge University

Purwanto, HS., Hidayat, W., Setiahadiwibowo, AP. (2020) Identification of Metal Sulfide Mineralization Zone using Time Domain Induced Polarization Method in Pakenjeng Region, Garut, West Java, Indonesia. *International Research Journal of Advanced Engineering and Science Vol 3, Issue 3.*

Prasetyadi, C., E.R., Suparka, A.H., Harsolumakso, dan B., Sapiie. (2006a): An overview of Paleogene stratigraphy of the Karangsambung area, Central Java: Discovery of a new type of Eocene rock, *Proceedings Jakarta 2006 International Geoscience Conference and Exhibition*, Jakarta.

Reynolds, J. M. (1997). *An Introduction to Applied and Environmental Geophysics*. Chichester: John Wiley and Sons Ltd. 796p.

Richards, L.A., Magnone, D., Sovann, C., Kong, C., Uhlemann, S., Kuras, O., van Dongen, B.E., Ballentine, C.J., Polya, D.A., 2017. H*igh-resolution profile of inorganic aqueous* *geochemistry and key redox zones in an arsenic bearing aquifer in Cambodia*. Sci. Total Environ. 590–591, 540–553

Sumner, J.L. (1976). Principle of Induced Polarization for Geophysical Interpretation, Elsevier, Amsterdam.

Telford, W.M., L.P. Geldart., R.E. Sheriff. (, 1990). *Applied Geophysics Second edition*. New York. Cambridge.

Uhlemann, S., Kuras, O, Richards, LA., Naden, E., Polya, D.A. (2017). Electrical resistivity tomography determines the spatial distribution of clay layer thickness and aquifer vulnerability, Kandal Province, Cambodia. *Journal of Asian Earth Sciences* 147 (2017) 402–414

VII. APPENDIX

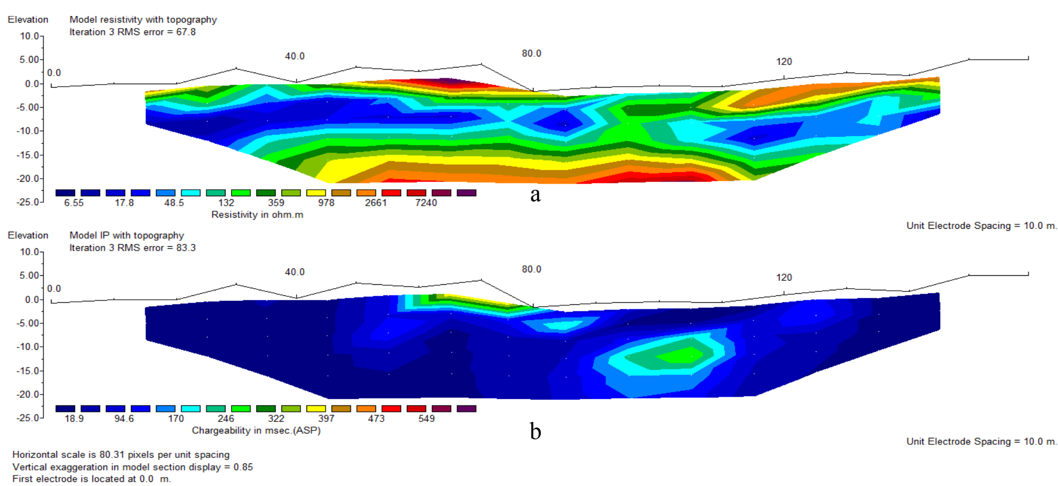

Figure 8. (a) The resistivity section (Ohm.m), (b) chargeability (msec) line 1 (space between electrodes 10 meter)

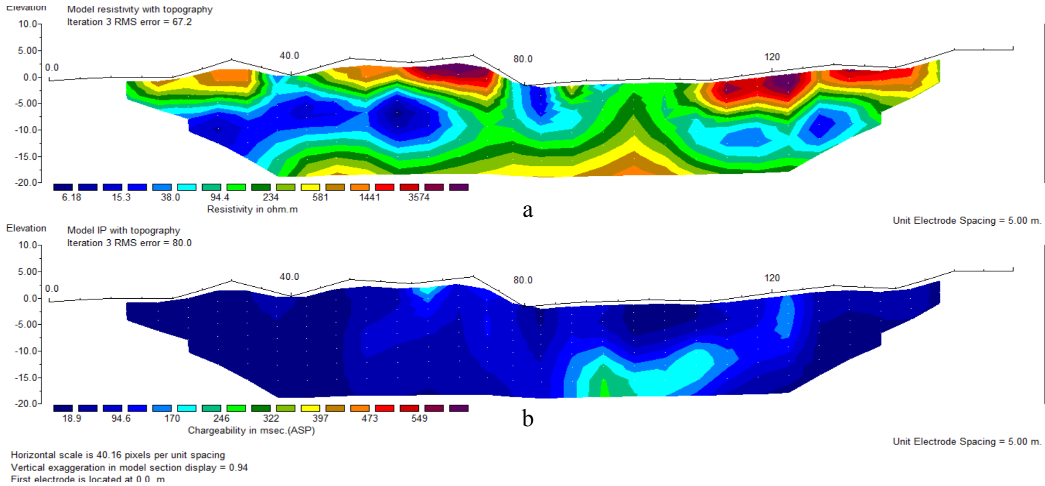

Figure 9. (a) The resistivity section (Ohm.m), (b) chargeability (msec) line 1 (space between electrodes 5 meter)

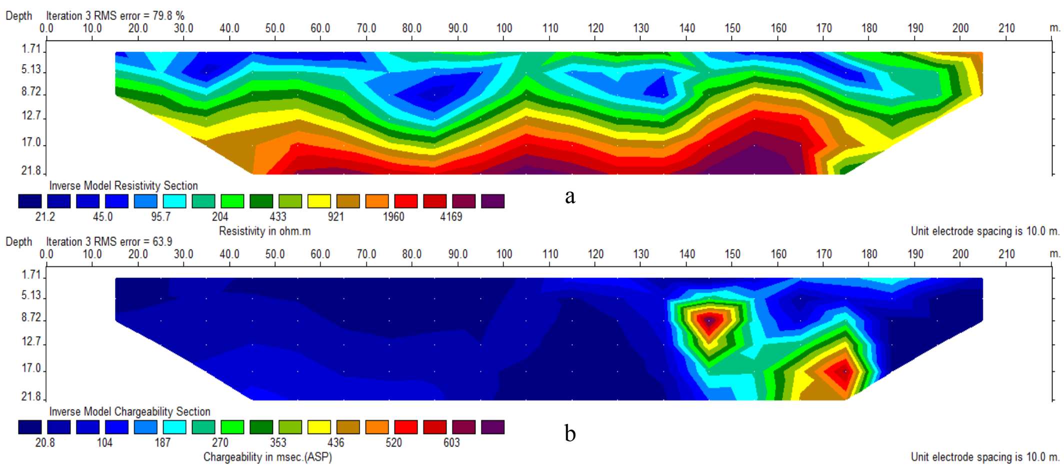

Figure 10. (a) The resistivity section (Ohm.m), (b) chargeability (msec) line 4 (space between electrodes 10 meter)

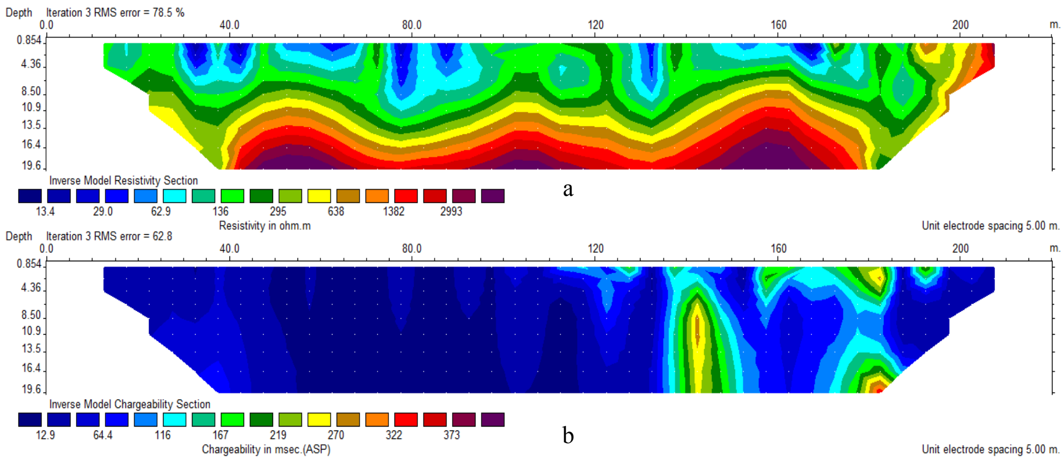

Figure 11. (a) The resistivity section (Ohm.m), (b) chargeability (msec) line 4 (space between electrodes 5 meter)